Discover Oncology

Research

PTTG1 promotes M2 macrophage polarization via the cGMP-PKG signaling pathway and facilitates EMT progression in human epithelial ovarian cancer cells

Liang Tian[1,3] · Liyun Liu[2] · Chunlou Wang[3] · Yan Kong[4] · Zhigang Miao[3] · Qing Yao[3] · He Zhang[3] · Yuehong Li[1]

Received: 5 February 2025 / Accepted: 25 April 2025
Published online: 12 May 2025

Abstract
Epithelial Ovarian Cancer (EOC) is complex and heterogeneous, making accurate prognosis and treatment prediction difficult. New therapeutic targets and their mechanisms are urgently needed. This study explored the role of PTTG1 in ovarian cancer via the cGMP-PKG signaling pathway, focusing on its effects on M2 macrophage polarization and EMT progression in EOC cells. Using the GSE135886 database, we performed differential gene expression, pathway enrichment, and immune infiltration analyses to identify key targets influencing EMT and macrophage polarization. We then constructed PTTG1 knockdown and overexpression cell lines to assess the impact of PTTG1 on cell proliferation, migration, invasion, EMT, and macrophage polarization in vitro. Analysis revealed that differentially expressed genes were enriched in the cGMP-PKG pathway and correlated with M2 macrophages. PTTG1 overexpression in A2780 and SK-OV-3 ovarian cancer cells promoted proliferation, invasion, and migration, while enhancing sGC, PKG1, and PKG2 expression to activate the cGMP-PKG pathway and induce M2 macrophage polarization. PTTG1 knockdown produced opposite results, reinforcing our conclusions. This study uncovers a novel mechanism of PTTG1 in ovarian cancer development and suggests it as a potential therapeutic target.

Keywords Ovarian cancer · PTTG1 · CGMP-PKG signaling pathway · Macrophage polarization · Epithelial-mesenchymal transition

1 Introduction

Ovarian cancer or primary ovarian cancer (POC) is a gynecological malignancy with the highest mortality rate worldwide and seriously threatens the health of women. According to the latest data from the World Health Organization, there will be over 300,000 new cases of POC and approximately 200, 000 deaths in 2022 [1, 2]. POC have diverse pathological types, mainly epithelial ovarian cancer (EOC), germ cell tumors, and sex cord-stromal tumors. Among these, EOC accounts for 80%–90% and is the predominant subtype [3]. The occurrence and development of EOC are complex and highly heterogeneous. Although progress has been made in monitoring, diagnosis, and management of the disease, the accurate prediction of prognosis and treatment effects remains a challenge. Therefore, the exploration of new therapeutic targets and their pathogenesis is urgently needed [4]. In this context, research on macrophage polarization and

✉ Yuehong Li, liyuehong1993@hebmu.edu.cn | [1]Department of Pathology, The Second Hospital of Hebei Medical University, No. 215, Heping West Road, Xinhua District, Shijiazhuang 050000, China. [2]Department of Pathology, Tangshan Gongren Hospital, Tangshan 063000, China. [3]Department of Pathology, Cangzhou Central Hospital, Cangzhou 061000, China. [4]Department of Clinical Lab, Cangzhou Central Hospital, Cangzhou 061000, China.

Fig. 1 Screening of differentially expressed genes in different grades of ovarian cancer in the GSE135886 database through the online database. **A** Principal component analysis (PCA) of dataset. **B** Heat map of the top differentially expressed genes. **C** Volcano plots of differentially expressed genes in different grades of ovarian cancer compared using pairwise comparisons. **D** Venn diagram of intersecting genes. **E** GO functional enrichment analysis of intersecting genes. **F** KEGG functional enrichment analysis of intersecting genes. **G** Analysis of differentially expressed genes in immune cells. **H** PPI analysis of differentially expressed genes related to macrophages

epithelial-mesenchymal transition (EMT) has shown great potential. Various factors secreted by M2 macrophages promote tumor proliferation, remodel the extracellular matrix, and inhibit the activity of immune cells, while EMT enhances the migration and invasion abilities of tumor cells [5]. Notably, factors secreted by M2 macrophages can induce EMT, which can also affect macrophage polarization, forming a positive feedback loop. This interaction may reveal new mechanisms and treatment strategies in the development of ovarian cancer [6].

Further in-depth exploration has revealed that cyclic guanosine 3′,5′-monophosphate (cGMP)-dependent protein kinase I (PKGI) plays a complex role in the development and occurrence of ovarian cancer. PKGI is activated upon binding to cGMP and can cause abnormal cell proliferation [7]. In other cancers, activation or overexpression of the cGMP-PKG pathway can stimulate the metastasis of breast cancer stem cells and malignant progression of cervical cancer tumors [8, 9], whereas activation of the cGMP-PKG pathway may inhibit cell apoptosis and promote cell proliferation in prostate cancer under the LPS—stimulated environment [10]. From this, it can be seen that the cGMP-PKG pathway has a dual-sided effect. Regarding its anti-tumor mechanism, the activation of the cGMP-PKG pathway may regulate the expression of inflammation-related factors, thereby altering the inflammatory microenvironment to make it unfavorable for cancer cell growth. For example, it may inhibit the production of pro-inflammatory cytokines such as tumor necrosis factor-α and interleukin-6. These cytokines can promote cancer cell proliferation, survival, and metastasis in the tumor microenvironment [11]. At the same time, this pathway may enhance the expression of anti-inflammatory factors, creating a microenvironment that relatively inhibits tumor growth. Additionally, the PKGI pathway is closely related to the EMT and macrophage polarization states. EMT is a key process in tumor progression and metastasis, involving the transformation of epithelial cells to mesenchymal cell phenotypes, and may affect the invasion and metastasis of esophageal squamous cell carcinoma by regulating the expression of EMT-related molecules [12]. Simultaneously, the polarization state of macrophages significantly influences the metastatic ability of ovarian cancer cells. Co-culture of M2 macrophages with ovarian cancer cells can enhance the invasion ability of the latter, which is related to increased expression of p-VASP, PKG1, and PKG2 [13]. Therefore, the cGMP-PKG pathway may play a crucial role in the progression of ovarian cancer by influencing EMT and macrophage polarization, thereby providing new therapeutic targets and research perspectives for the treatment of ovarian cancer.

Based on the current research status, we downloaded the GSE135886 database to explore differential gene expression, pathway enrichment, and immune infiltration in different grades of ovarian cancer samples to identify key targets affecting EMT and macrophage polarization. Finally, we focused on PTTG1. PTTG1 has been identified as an oncogene in various cancers [14–16]. In ovarian cancer, PTTG1 has been recognized as an ovarian cancer biomarker [17], and high expression of PTTG1 has been associated with angiogenesis in ovarian tumors [18]. Dataset analysis showed that the differentially expressed genes were significantly associated with M2 macrophages. However, the correlation between PTTG1 and macrophage polarization in ovarian cancer has not been reported. We constructed PTTG1 knockdown and overexpression cell lines to evaluate the effects of high and low expression of PTTG1 on in vitro cell proliferation, migration, invasion, epithelial-mesenchymal transition (EMT), and macrophage polarization. This study provides a new mechanism for the role of PTTG1 in the development and progression of ovarian cancer, deepens our understanding of the complex biological characteristics of ovarian cancer, and offers a scientific basis for the development of new treatment strategies.

2 Materials and methods

2.1 Differential gene analysis of the GSE135886 dataset

Ovarian cancer-related datasets were retrieved from the public GEO database Gene Expression Omnibus (https://www.ncbi.nlm.nih.gov/geo/) and the GSE135886 dataset was used for analyses. Ovarian cancer tumor tissues and adjacent control samples in the dataset were selected to explore the differential expression of high-grade ovarian cancer samples (High_Grade), low-grade ovarian cancer samples (Low_Grade), and controls (Ctrl). The R packages"FactoMineR"and"fact

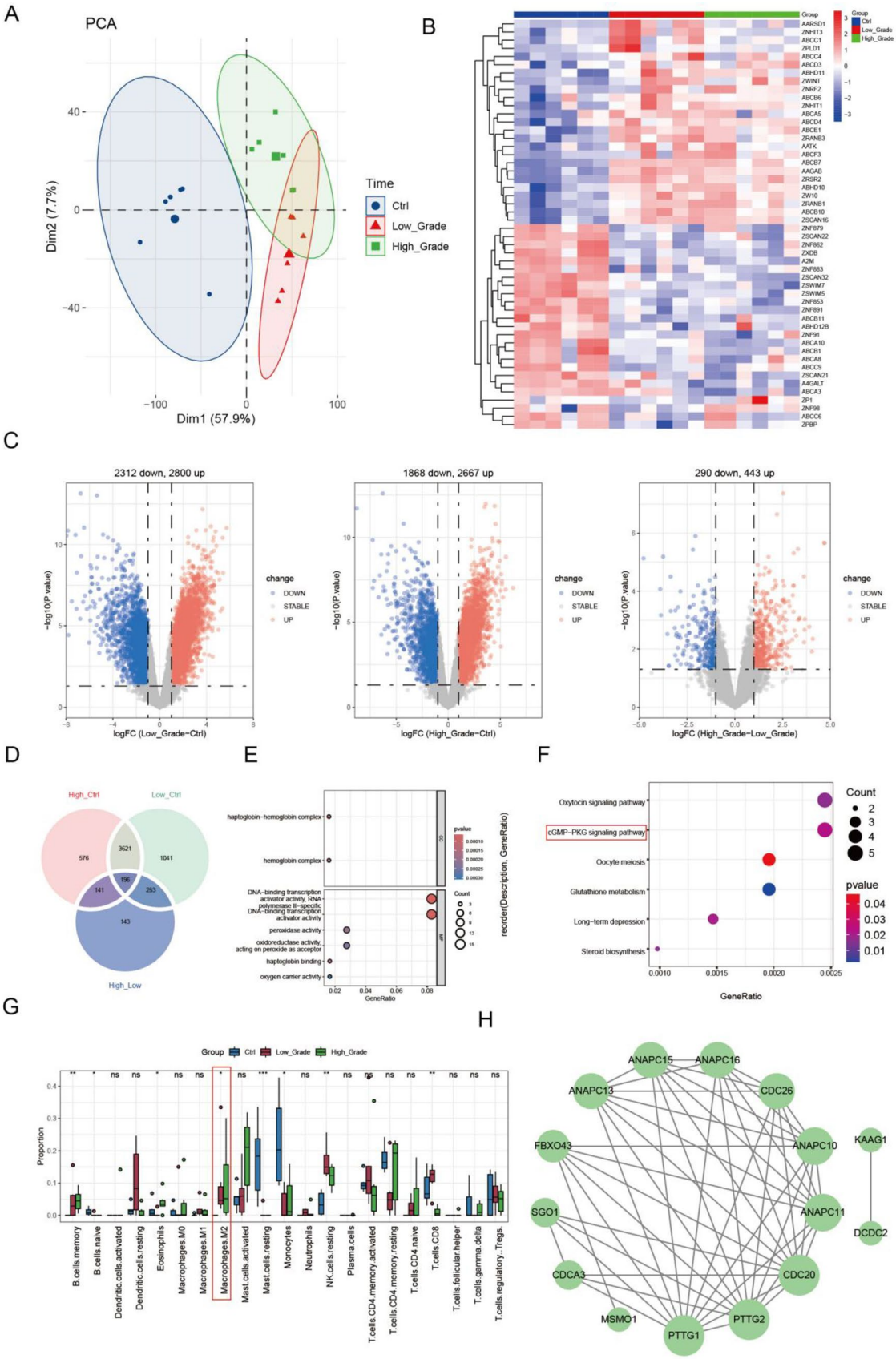
A
PCA
Dim2 (7.7%)
Dim1 (57.9%)
Time
Ctrl
Low_Grade
High_Grade
B
Group
Ctrl
Low_Grade
High_Grade
C
2312 down, 2800 up
1868 down, 2667 up
290 down, 443 up
change
DOWN
STABLE
UP
-log10(P.value)
logFC (Low_Grade−Ctrl)
logFC (High_Grade−Ctrl)
logFC (High_Grade−Low_Grade)
D
High_Ctrl
Low_Ctrl
High_Low
576
3621
1041
196
141
253
143
E
haptoglobin−hemoglobin complex
hemoglobin complex
DNA−binding transcription activator activity, RNA polymerase II−specific
DNA−binding transcription activator activity
peroxidase activity
oxidoreductase activity, acting on peroxide as acceptor
haptoglobin binding
oxygen carrier activity
pvalue
Count
GeneRatio
reorder(Description, GeneRatio)
F
Oxytocin signaling pathway
cGMP−PKG signaling pathway
Oocyte meiosis
Glutathione metabolism
Long−term depression
Steroid biosynthesis
Count
pvalue
GeneRatio
G
Group
Ctrl
Low_Grade
High_Grade
Proportion
B.cells.memory
B.cells.naive
Dendritic.cells.activated
Dendritic.cells.resting
Eosinophils
Macrophages.M0
Macrophages.M1
Macrophages.M2
Mast.cells.activated
Mast.cells.resting
Monocytes
Neutrophils
NK.cells.resting
Plasma.cells
T.cells.CD4.memory.activated
T.cells.CD4.memory.resting
T.cells.CD4.naive
T.cells.CD8
T.cells.follicular.helper
T.cells.gamma.delta
T.cells.regulatory..Tregs.
H
ANAPC15
ANAPC16
ANAPC13
CDC26
FBXO43
ANAPC10
KAAG1
SGO1
ANAPC11
DCDC2
CDCA3
CDC20
MSMO1
PTTG2
PTTG1

oextra"were used to perform principal component analysis (PCA) on different grouped samples. The results are shown in Fig. 1. The PCA results showed that the different groups were organized into different clusters. The"limma"package was used for differential expression analysis of different groups. Screening was performed according to |logFC|> 1 and $p < 0.05$. Volcano plots and heat maps were drawn for differentially expressed genes in different groups. Grouping information: The mRNA expression data of GSE135886 were extracted, with the number of samples for High_Grade, Low_Grade, and control being 6:6:6. Differential expression analysis group comparisons: High_Grade VS control, low-grade VS control, and high-grade vs. low-grade The R package"VennDiagram"was used to analyze the High_Grade, Low_Grade, and control samples to determine the intersection of differential genes.

2.2 GO and KEGG functional enrichment of differential intersection genes

To explore the enrichment of differential gene pathways in ovarian cancers of different grades, we conducted KEGG and GO functional enrichment analyses to observe the enrichment of differential genes. A Venn diagram was drawn for the intersection of differential genes obtained from the differential analysis of different groups. For the differential intersection genes, GO and KEGG functional enrichments were performed using the R package"clusterProfiler," and the top-ranked results were displayed.

2.3 Analysis of immune cells and macrophage differential genes

We also focused on the relationship between the intersection genes and the infiltration levels of immune cells. CIBERSORT was used to analyze 22 immune cell types in GSE135886. Immune cells with an abundance of zero in all samples were removed, and the relative abundance of immune cells in different groups was tested using the Kruskal–Wallis test. Pearson's correlation analysis was performed based on the relative abundance of the aforementioned macrophages (M0, M1, and M2) and the intersecting genes obtained earlier. According to |cor|> 0.5 & pvalue < 0.05, the STRING database (https://cn.string-db.org/) was used to construct the Protein–Protein Interaction Networks (PPI) based on the aforementioned M2 macrophage-related genes and visualized using Cytoscape 3.9.1.

2.4 Cell culture

Human ovarian cancer cell lines A2780 and SK-OV-3 and the human macrophage cell line THP-1 were purchased from Procell Life Science & Technology Co., Ltd. (Wuhan, China). Cells were cultured in 1640 medium (SH30027.01, HyClone, China) containing 10% fetal bovine serum (C0229, Beyotime Biotech Inc, China) and 1% penicillin–streptomycin mixture (C0222, Beyotime Biotech Inc, China), and cells were cultured in an incubator (Jiemei Electronics, CI-191 C) at 37 °C and 5% CO_2. The medium was changed every other day, and the cells were used for subsequent studies after entering the exponential growth phase.

2.5 Construction of PTTG1 downregulation and overexpression cell lines

To confirm the impact of high and low PTTG1 expression on the EMT process in ovarian cancer cells, macrophage M2 polarization, and the cGMP-PKG signaling pathway, we established PTTG1 knockdown and over—expression cell lines in A2780 and SK-OV-3 cells. We selected human ovarian cancer cells A2780 and SK-OV-3 that were in the exponential growth phase. Specific siRNAs targeting PTTG1 were designed and synthesized. Using liposome transfection reagents, siRNAs were transfected into A2780 and SK-OV-3 cells, according to the manufacturer's instructions. After 72 h of transfection, the expression level of PTTG1 was detected using RT-qPCR and Western blotting to verify the knockdown effect. For subsequent experiments, the knockdown cell lines were divided into three groups: siNC (Small interfering RNA negative control), siPTTG1-1, and siPTTG1-2. We constructed an overexpression plasmid containing PTTG1. Transfection was performed when the cells reached an appropriate density and the plasmid was transfected into the cells using the corresponding transfection reagent. After transfection, stably expressing cell lines were screened for resistance, and the effect of PTTG1 overexpression was verified by RT-qPCR and Western blotting. In subsequent experiments, overexpressing cell lines were divided into two groups: vector and oePTTG1. The sequences of the siRNAs and overexpression plasmids are listed in Table 1.

2.6 Induction of M0 and M2 differentiation of THP-1 cells and co-culture system

Induction of THP-1 cell differentiation into macrophages: THP-1 cells were stimulated with phorbol ester (PMA; HY-18739, MedChemExpress, China) to induce their differentiation into macrophages. PMA was added to the medium at a final concentration of 150 ng/ml and incubated for 48 h [19]. After differentiation, 20 ng/ml IL-4 (P5129; Beyotime Biotech Inc., China) and 20 ng/ml IL-13 (P5178; Beyotime Biotech Inc., China) were added as described previously and cultured for another 48 h to induce macrophage polarization to the M2 type [20]. Human ovarian cancer cell lines A2780 and SK-OV-3 were inoculated into the lower chamber of the Transwell, and THP-1 cells were inoculated into the upper chamber of the transwell to achieve a co-incubation system [21].

2.7 CCK8 assay

To verify the impact of PTTG1 on cell viability, the Cell Counting Kit-8 (CCK-8) assay was utilized to examine how high and low levels of PTTG1 expression affect cell viability. Cells were treated as required by the different groups. A2780 and SK-OV-3 cell lines in the exponential growth phase were collected, trypsin (P4021, Beyotime Biotech Inc., China) was added to digest the cells, centrifuged at 1200 g for 3 min. The cell supernatant was discarded, and 1640 culture medium was added to resuspend the cells. Cell density was calculated using a cell counter (SCC-M630, Wuhan Servicebio Technology Co., Ltd, China), and 2.5×10^3 cells were inoculated in each well of a 96-well plate and cultured in a cell incubator for 0, 24, 48, and 72 h. After incubation, 10 uL of CCK8 solution (C0039, Beyotime Biotech Inc, China) was added to each well and incubated for another 2 h. The 96-well plate was then removed, and the absorbance at OD450 was detected using a SuPerMax 2500 L microplate reader (Shanghai Shanpu Biotechnology Company, China).

2.8 Plate clone formation assay

To verify the effect of PTTG1 on cell proliferation ability, the CCK8 assay was used to detect the impact of high and low PTTG1 expression on cell proliferation. Cells were treated as required by the different groups. Cell digestion and counting were performed as described previously. A2780 and SK-OV-3 cells were inoculated in a six-well plate at a density of 300 cells/well and incubated for 9 days. The medium was changed every two days. After incubation, the medium was aspirated, and the cells were washed three times with PBS. A fixative solution (P0099; Beyotime Biotech Inc., China) was added and incubated for 30 min. The fixative solution was discarded and 0.5% crystal violet solution (C0121, Beyotime Biotech Inc., China) was added and incubated for 15 min. After incubation, excess liquid was washed away with PBS, and the cells were air-dried. Images were captured and saved, and the number of cell clones was calculated using ImageJ 1.5.2a.

2.9 Cell scratch assay

To verify the impact of high and low expression levels of PTTG1 on the cell migration ability, we employed the Transwell method to detect the alterations in cell invasion ability. Cells were treated as required by the different groups. Cell

Table 1 RT-qPCR primer information and sequence information related to knockdown and overexpression

Gene	Forward primer (5′–3′)	Reverse primer (5′–3′)
CD206	GGGTTGCTATCACTCTCTATGC	TTTCTTGTCTGTTGCCGTAGTT
CD163	TTTGTCAACTTGAGTCCCTTCAC	TCCCGCTACACTTGTTTTCAC
GAPDH	CTGGGCTACACTGAGCACC	AAGTGGTCGTTGAGGGCAATG
Gene	SS Sequence	AS Sequence
SiNC	UUCUCCGAACGUGUCACGUUU	ACGUGACAGGUUCGGAGAAUU
SiPTTG1-1	GGGAGAUCUCAAGUUUCAACA	UUGAAACUUGAGAUCUCCCAU
SiPTTG1-2	GACUGAGAAGACUGUUAAAGC	UUUAACAGUCUUCUCAGUCAU
SiPTTG1-3	GGAACUGUCAACAGAGCUACA	UAGCUCUGUUGACAGUUCCCA
Gene	Primer sequence (5′–3′)	
pcDNA3.1-PTTG1-F	GTACCGAGCTCGGATCCATGGCTACTCTGATCTATG	
pcDNA3.1-PTTG1-R	GATATCTGCAGAATTCTTAAATATCTATGTCACAGC	

digestion and counting were performed as described previously. A2780 and SK-OV-3 cells were seeded in six-well plates at a density of 3×10^5 cells/well. The next day, a sterile 10 µL pipette tip was used to make a scratch on the cell monolayer. The old medium was discarded, and the fallen cells were gently washed with PBS. The six-well plate was taken out at 0 and 48 h, and the scratch width at the same position was observed under a microscope and photographed. Images were used to calculate the cell migration ratio using Image J 1.5.2a.

2.10 Transwell assay

To confirm the impact of high and low expression of PTTG1 on the cell invasion ability, the changes in cell invasion ability were detected through the Transwell assay.

The Swe matrix gel (G4131; Wuhan Servicebio Technology Co., Ltd., China) was removed and the matrix gel was diluted eight times with serum-free 1640 medium. Fifty microliters of matrix gel were added to the upper chamber of the Transwell plate and incubated for 3 h. 300 µL of 1640 medium containing 20% FBS was added to each well in the lower chamber of the Transwell for later use. Cells were treated as required by the different groups. Cell digestion and counting were performed as described previously. A2780 or SK-OV-3 cells were inoculated in the upper chamber of a transwell plate at a density of 1×10^4 cells/well and incubated for 18 h. After incubation, 1 mL of the cell fixative was added to each well and incubated for 30 min. The fixative was washed with PBS and 1 mL of 1% crystal violet solution was added to each well and incubated for 5 min. The crystal violet solution was washed off with tap water, and the cells in the upper chamber were wiped with a cotton swab, air-dried, and photographed under a microscope. Images were used to calculate the number of invasive cells using ImageJ 1.5.2 a software.

2.11 RT-qPCR assay

To verify whether the PTTG1 knockdown and over-expression cell lines were successfully constructed and to examine the changes in M2 macrophage polarization markers, the expression changes of related factors at the mRNA level were detected by RT-qPCR. Cells were treated as required by the different groups. Cell digestion and counting were performed as described previously. Total RNA was extracted using an RNA extraction kit (R0017M; Beyotime Biotech Inc., Shanghai, China). The concentration and purity of RNA were determined using a NanoDrop™ Eight spectrophotometer (912 A1101, Thermo Fisher Scientific, China). cDNA was obtained using the RevertAid RT Reverse Transcription Kit (D7168L; Beyotime Biotech Inc., China). Specific primers for the target mRNA were designed and synthesized. The reaction system was prepared in a qPCR tube and included cDNA, primers, fluorescent dye, and a PCR solution. The reaction tubes were placed in a QuantStudio™ 7 Pro real-time fluorescence quantitative PCR instrument (A43169, Thermo Fisher Scientific, China). Pre-denaturation was set at 95 °C for 2 min, followed by 40 cycles of 95 °C for 13 s and 60 °C for 32 s. Melting curve analysis was performed at 95 °C for 15 s, 56 °C for 15 s, and 95 °C for 15 s. GAPDH was used as an internal reference, and the relative expression level of the target mRNA was calculated using the 2^(-ΔΔCt) method. The RT-qPCR primer sequences are listed in Table 1.

2.12 Flow cytometry

To detect the changes in the expression of macrophage polarization-related markers, the expression levels of CD206 and CD163 were measured by flow cytometry. Cells were treated as required by the different groups. Digestion and centrifugation were performed as previously described to obtain A2780 and SK-OV-3 cell pellets. An appropriate amount of fluorescently labeled monoclonal antibody against CD206 was added to one tube, and an appropriate amount of fluorescently labeled monoclonal antibody against CD163 was added to the other tube. The mixture was gently shaken and incubated at room temperature in the dark for a certain period. After incubation, the cells were washed with an appropriate amount of PBS and unbound antibodies were removed. After centrifugation to remove the supernatant, the cells were resuspended in PBS. Finally, flow cytometry was used for detection and a fluorescence signal was obtained. Changes in the expression levels of CD206 and CD163 were analyzed using Flow Jo software. Antibody information is detailed in Table 2.

2.13 Western blot experiment

To detect the changes in proteins related to the cGMP—PKG pathway as well as proteins related to macrophage polarization (CD163 and CD206), Western blot was used to examine the alterations in these proteins under high and low PTTG1 expression levels. Cell digestion was performed as described previously. Suspensions of A2780 and SK-OV-3 cells were collected and centrifuged at 2000 × g for 5 min. The supernatant was discarded, and cell lysis buffer (G2002, Wuhan Servicebio Technology Co., Ltd, China) was added and incubated on ice for 30 min. The protein concentration was determined using a BCA kit (G2026, Wuhan Servicebio Technology Co., Ltd, China). After determining the protein concentration, cell lysis buffer and 5 × Loading Buffer (G2075, Wuhan Servicebio Technology Co., Ltd, China) were added to adjust the concentration of each single-labeled sample for consistency. The mixture was boiled in a water bath for 15 min to denature the proteins. Equal amounts of protein solution and molecular weight markers were added, and electrophoresis was performed at 120 V for 90 min. Proteins were transferred from the gel to a NC or PVDF membrane using the wet transfer method at a constant current of 260 mA for 60 min. After the transfer, the membranes were incubated with 5% skim milk powder for 1 h. Primary antibodies were added and incubated overnight at 4 °C. The primary antibody, and the corresponding secondary antibody was added and incubated for 2 h. After thorough washing with TBST, the bands were visualized using an ECL chemiluminescence solution (G2014, Wuhan Servicebio Technology Co., Ltd, China), and the target bands were analyzed using ImageJ software with GAPDH as the internal reference. The gray value of the protein bands was analyzed using ImageJ 1.5.2a software, and the relative expression level of the target protein was calculated with β-actin as the internal reference. Antibody information and dilution ratios are presented in Table 2.

2.14 Statistical analysis

All experimental procedures involved in this study were independently repeated at least three times. Experimental data were presented in the standard format of scientific reporting, expressed as mean ± standard deviation (mean ± standard deviation, SD). In terms of statistical analysis, when comparing potential differences between two groups of data, Student's unpaired t-test was selected in this study. For comparisons involving more than two experimental groups, a one-way analysis of variance (ANOVA) was used, followed by Tukey's post-hoc test for multiple comparison corrections. All statistical analyses were accomplished using GraphPad Prism 9.5 software.

Table 2 Antibody information used in this study

Gene name	Manufacturer	Article number	Dilution ratio
CD206	BioLegend	141706	10^6 cells/5 μL
CD163	BioLegend	155208	10^6 cells/5 μL
CD206	Affinity	DF4149	1:1000
CD163	BOSTER	A00812-2	1:2000
sGC	Affinity	AF0619	1:1000
PTTG1	HUABIO	ET7107-50	1:500
PKG2	Affinity	DF3257	1:1000
PKG1	BOSTER	A01708-3	1:1000
GAPDH	HUABIO	ET1601-4	1:10000
Goat Anti-Rabbit IgG H&L (HRP)	abcam	ab6721	1:10000
Goat Anti-Mouse IgG H&L (HRP)	abcam	ab6789	1:10000

3 Results

3.1 PTTG1 was identified as a candidate differential gene related to macrophage M2 polarization

To screen out the differentially expressed genes related to the progression of ovarian cancer, we used the online dataset GSE135886 to explore the differential expression of high-grade ovarian cancer samples (High_Grade), low-grade ovarian cancer samples (Low_Grade), and controls (Ctrl). Principal component analysis was performed on the differentially expressed genes. A total of 4535 differential expression genes were obtained in the High_Grade VS Ctrl group, with 2667 up-regulated and 1868 down-regulated. A total of 5112 expression genes were identified in the Low_Grade VS Ctrl group, with 2800 upregulated and 2312 downregulated genes. A total of 733 expression genes were identified in the High_Grade VS Low_Grade group, with 443 upregulated and 290 downregulated genes, as shown in Fig. 1A. Heatmap analysis of differential genes showed that AARSD1, ZNHIT3, and ABCC1 were abnormally expressed in ovarian cancer, whereas ZPBP, ABCC6, and ZNF98 were expressed at low levels. However, these genes did not show obvious gradient expression differences between low- and high-grade tumors (Fig. 1B). Volcano plots of the DEGs in the different groups are shown in Fig. 1C. The Venn diagram shows 196 intersecting genes in the different groups (Fig. 1D). GO (Fig. 1E) and KEGG (Fig. 1F) functional enrichment analyses of the intersecting genes showed that they were mainly enriched in the cGMP-PKG signaling pathway. Therefore, we explored the cGMP-PKG signaling pathway. The results of the immune cell differential gene analysis showed significant differences in M2 macrophages, B cells, and mast cells (Fig. 1G). In this study, we focused on M2 macrophages. To further explore the differentially expressed genes affecting macrophage M2 polarization in ovarian cancer, we screened 29 genes with strong correlations with M2 macrophages and found that ANAPC13, 15, 16, 10, 11, CDC20, 26, PTTG1, and PTTG2 had more interactions (Fig. 1H). Considering the above proteins as priorities, a search through Pubmed using"Cancer,""macrophage," and"gene name"revealed that only PTTG1 had one related study. Therefore, in subsequent studies, we considered PTTG1 as the main research target.

3.2 PTTG1 can promote the proliferation, invasion, and migration of A2780 and SK-OV-3 cells

To verify the effect of PTTG1 expression on ovarian cancer cells, we constructed PTTG1 knockdown and overexpression cell lines to detect changes in the proliferation, invasion, and migration of ovarian cancer cells. Western blotting and RT-qPCR results showed that, in A2780 and SK-OV-3 cells, siPTTG1-1 and siPTTG1-2 significantly downregulated the relative expression levels of PTTG1 mRNA and protein, whereas oe-PTTG1 significantly upregulated the relative expression levels of PTTG1 mRNA and protein. These results confirmed that we successfully constructed PTTG1 up-regulation and down-regulation in A2780 and SK-OV-3 cells, respectively (Fig. 2A and B). The CCK8 assay results indicated that compared with the siNC group, the siPTTG1-1 and siPTTG1-2 groups significantly inhibited the proliferation ability of the cells; conversely, the oe-PTTG1 group showed significantly enhanced proliferation ability compared to the vector group, and both were time-dependent, with a stronger regulatory effect as the action time increased. The results of the plate colony formation assay were consistent with those of the CCK8 assay (Fig. 3A). The number of clones formed by the siPTTG1-1 and siPTTG1-2 groups was significantly less than that of the siNC group, reflecting a significant decrease in their proliferation ability. The number of clones formed by the oe-PTTG1 group was significantly higher than that of the vector group, further confirming the enhancement of its proliferation ability (Fig. 3B). The cell scratch assay results showed that compared to the siNC group, the cell migration ability of the siPTTG1-1 and siPTTG1-2 groups was significantly weakened, and the scratch healing speed was significantly reduced. Transwell assays indicated that the number of cells passing through the chambers in the siPTTG1-1 and siPTTG1-2 groups was significantly lower than that in the siNC group, indicating that their invasive ability was significantly inhibited. Conversely, compared to the vector group, the oe-PTTG1 group showed significantly faster cell migration, faster scratch healing, and a significantly higher number of cells passing through the Transwell chambers, fully demonstrating the significantly enhanced cell invasion and migration abilities of the oe-PTTG1 group (Figs. 3C and 3D). In conclusion, these experimental results clearly reveal that PTTG1 plays an important role in promoting the proliferation, invasion, and migration of A2780 and SK-OV-3 cells, providing valuable experimental evidence for further understanding the occurrence and development mechanisms of ovarian cancer.

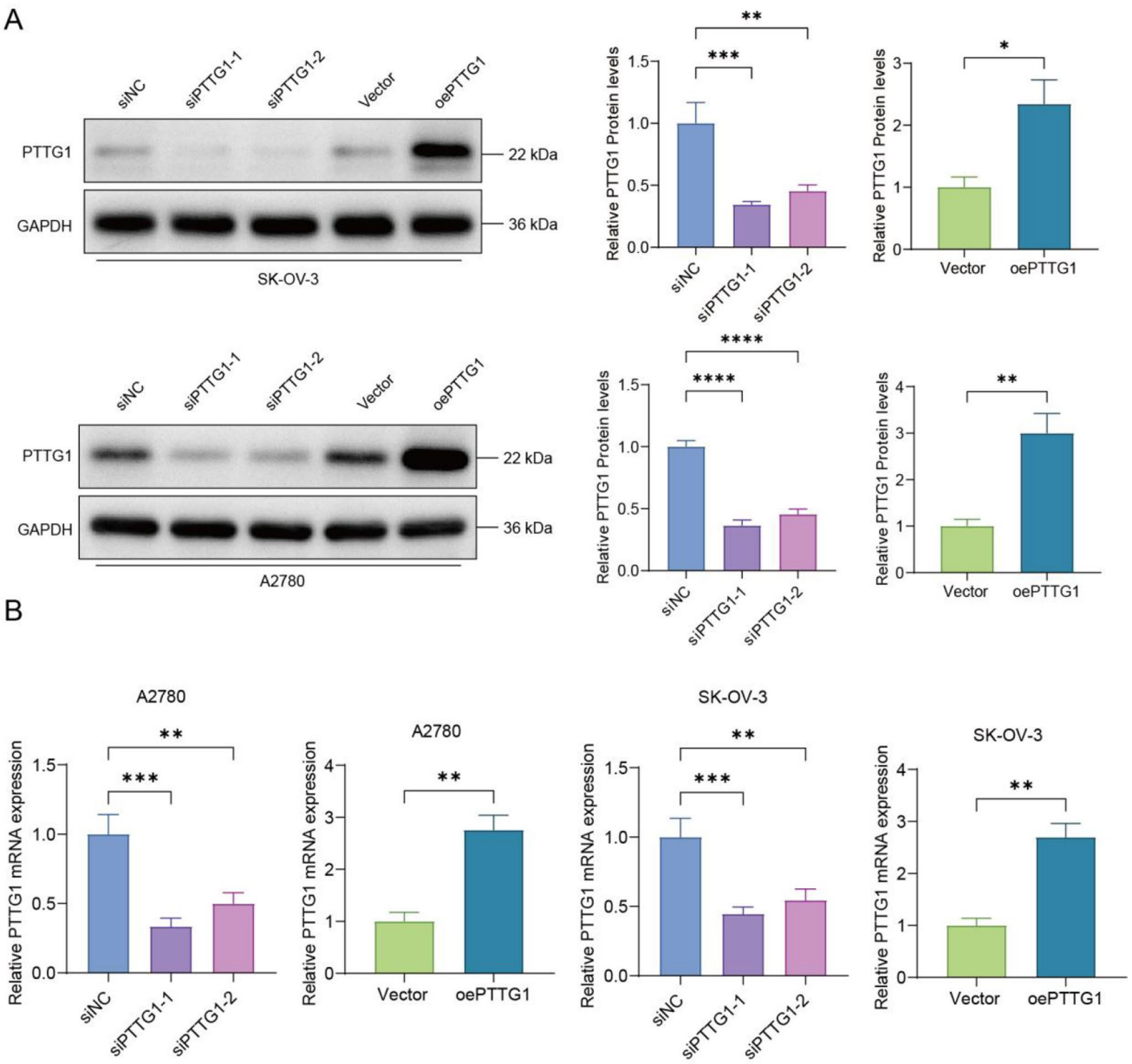

Fig. 2 Construction of PTTG1 overexpression and knockdown cell lines. Transfection with overexpression vectors and siRNA sequences in SK-OV-3 and A2780 cells and incubation for 48 h. **A** Relative expression of PTTG1 protein was detected by western blotting. **B** Detection of relative expression levels of PTTG1 mRNA by RT-qPCR. (Compared between the two groups, *P < 0.05, **P < 0.01, ***P < 0.001, ****P < 0.0001)

3.3 PTTG1 can induce the activation of the cGMP-PKG signaling pathway

In the aforementioned experiments, we clearly revealed the significant effects of PTTG1 on the proliferation, invasion, and migration abilities of A2780 and SK-OV-3 cells. To further explore the underlying molecular mechanism of action of PTTG1, we focused on detecting the regulatory effect of PTTG1 on the cGMP-PKG signaling pathway. Protein expression levels in the different treatment groups were detected by western blotting. The results clearly showed that, compared to the siNC group, the relative expression levels of sGC, PTTG1, PKG1, and PKG2 proteins in the siPTTG1-1 and siPTTG1-2 groups were significantly decreased. In contrast, compared to the vector group, the relative expression levels of these proteins in the oe-PTTG1 group were significantly increased. This result strongly confirms that PTTG1

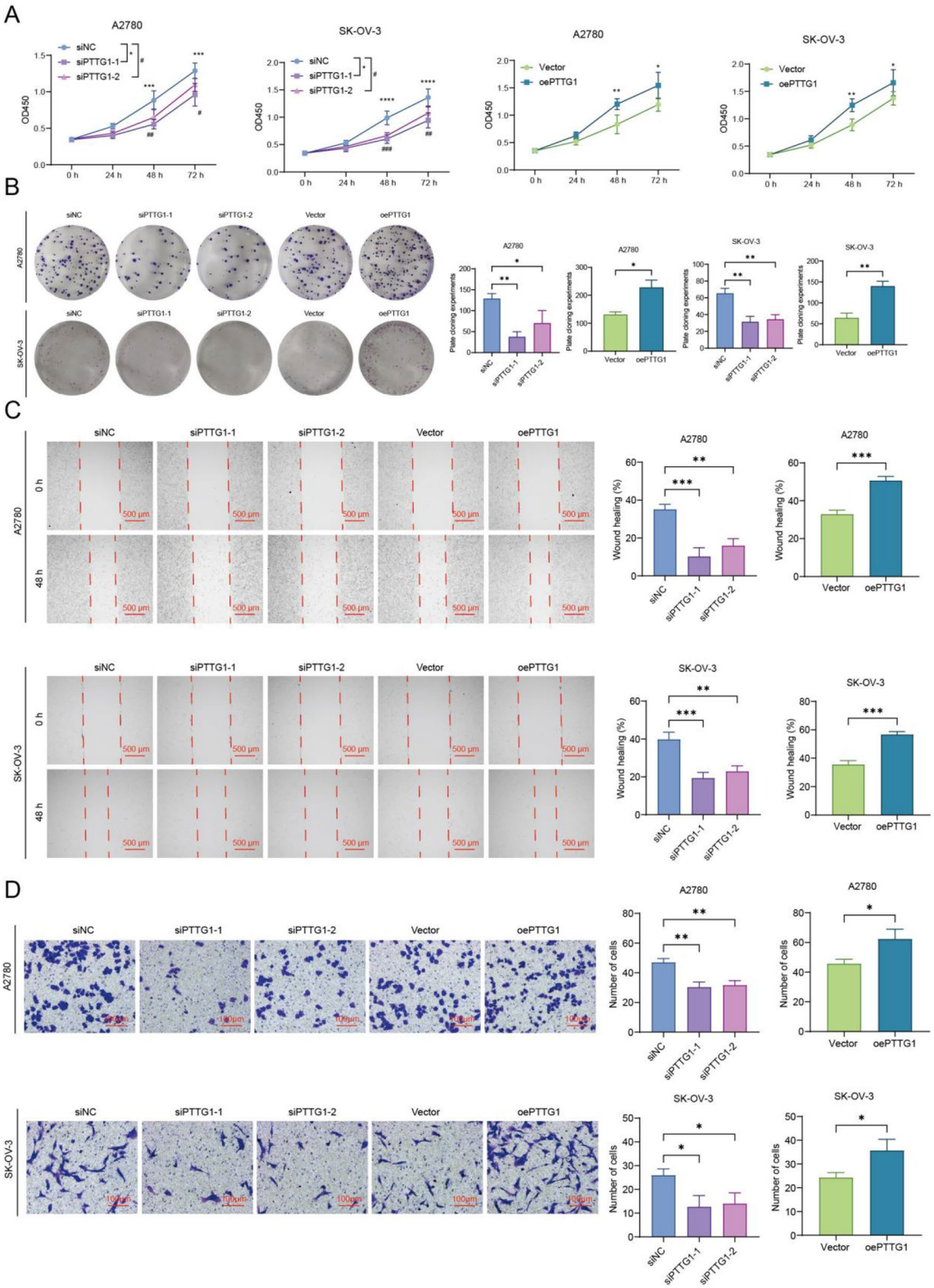

Fig. 3 PTTG1 can induce proliferation, invasion and migration of ovarian cancer cells. **A** Transfection of overexpression vectors and siRNA sequences in SK-OV-3 and A2780 cells, incubation for 0, 24, 48, and 72 h, and detection of changes in cell viability the CCK8 experiment. **B** Detection of changes in the proliferative ability of SK-OV-3 and A2780 cells using a plate clone formation experiment. **C** Changes in the migration abilities of SK-OV-3 and A2780 cells were detected using a cell scratch experiment. **D** Detection of changes in the invasion ability of SK-OV-3 and A2780 cells by transwell assay

can activate the cGMP-PKG signaling pathway, providing crucial experimental evidence for further understanding the intracellular mechanism of action of PTTG1 and its association with related signaling pathways (Fig. 4).

3.4 PTTG1 can induce M2 polarization of tumor-associated macrophages

We successfully confirmed the activating effect of PTTG1 on the cGMP-PKG signaling pathway. To comprehensively analyze the influence of PTTG1 on the tumor microenvironment, we further examined the changes in the M2 polarization of tumor-associated macrophages. We detected changes in the relative expression levels of CD206 and CD163 using flow cytometry, RT-qPCR, and Western blotting. The results showed that the downregulation of PTTG1 increased the proportion of positive cells of CD206 and CD163, inhibited the relative expression levels of mRNA and protein, while the overexpression of PTTG1 reduced the proportion of positive cells of CD206 and CD163 and enhanced the relative expression levels of mRNA and protein. The experimental results indicated that when PTTG1 was downregulated, the expression levels of CD206 and CD163 were significantly inhibited, whereas when PTTG1 was overexpressed, the expression levels of CD206 and CD163 were significantly increased (Fig. 5, Fig. 6A and B). This finding revealed that PTTG1 induced the role of inducing M2 polarization of macrophages.

4 Discussion

This study was conducted because EOC, the predominant subtype of POC, has a high degree of heterogeneity and a complex occurrence and development process, making accurate prediction of prognosis and treatment effects challenging[9]. Therefore, exploration of new therapeutic targets and their pathogenesis is urgently needed. This study focused on the mechanism of action of PTTG1 in ovarian cancer and achieved significant results in a series of experiments. In terms of the current research status at home and abroad, the mechanism of occurrence and development of ovarian cancer has always been one of the hotspots in the field of tumor research, but the specific role of PTTG1 in it has not been fully clarified. Previous studies have revealed some genes and signaling pathways related to ovarian cancer; however, our research provides new perspectives and evidence regarding the relationship between PTTG1, the cGMP-PKG signaling pathway, and macrophage M2 polarization.

Our experiments revealed that PTTG1, as a key factor, can promote the proliferation, invasion, and migration of A2780 and SK-OV-3 cells, which is somewhat similar to the research results of PTTG1 in other cancers[22]; however, the unique mechanism of action of PTTG1 still requires in-depth exploration. Moreover, the relationship between PTTG1 and the cGMP-PKG signaling pathway has not yet been reported. Methods to activate the cGMP-PKG signaling pathway include the use of cGMP analogs, sGC activators, PKG agonists, and gene therapy strategies, which are achieved by increasing cGMP production or directly activating PKG [23–25]. The degradation of cGMP is mainly mediated by specific members of the phosphodiesterase (PDE) family, especially PDE5. Its inhibitors, such as sildenafil, can indirectly increase cGMP levels by reducing cGMP degradation, thereby activating PKG [26]. In the present study, we experimentally confirmed that PTTG1 activates the cGMP-PKG signaling pathway. By confirming that PTTG1 enhances the expression levels of sGC, PKG2, and PKG1 proteins to activate the cGMP-PKG signaling pathway, we have discovered new targets for the targeted activation of the cGMP-PKG signaling pathway.

In addition, database exploration revealed that PTTG1 has a poor prognosis in liver cancer, and immune infiltration analysis showed a significant correlation with macrophage polarization, similar to our findings [27, 28]. Subsequently, we found that PTTG1 could enhance the expression levels of CD163 and CD206. As key phenotypic markers of M2 polarization, CD206 and CD163 are functionally complementary. CD206 mediates immunosuppressive endocytosis by recognizing pathogen- associated molecular patterns and is involved in tumor stroma remodeling [29]. On the other hand, CD163 activates the IL-10/STAT3 anti-inflammatory pathway by clearing the hemoglobin-haptoglobin complex, coordinately inhibiting the Th1-type immune response [30, 31]. It is worth noting that although both are regulated by classical M2—polarizing factors such as IL-4/IL-13, their expression patterns exhibit significant heterogeneity [32]. Research indicates that the expression of CD163 is more dependent on the activation of the glucocorticoid and TGF-β signaling pathways [33], while the up—regulation of CD206 is closely related to the PPARγ pathway [34] This difference suggests that the tumor microenvironment may coordinate their co-expression through a multi-dimensional signaling network. In this experiment, the knockout of PTTG1 led to a synchronous down—regulation of CD206 and CD163, implying that it may indirectly affect the polarization direction of macrophages by regulating EMT-related pathways (such as the cGMP-PKG signaling pathway). PTTG1 enhances cancer stemness in breast cancer and promotes the M2

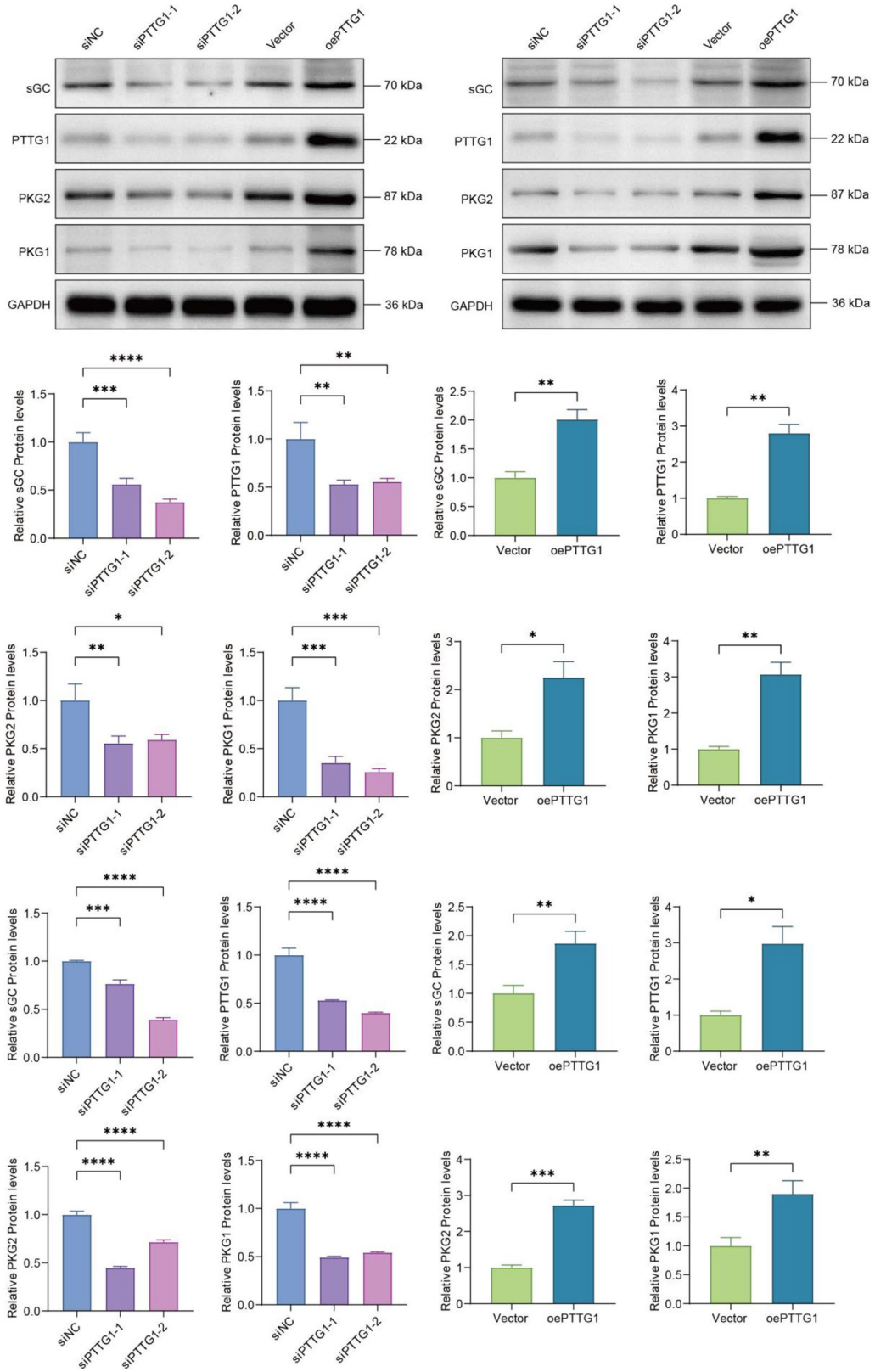

Fig. 4 PTTG1 can activate the cGMP-PKG signaling pathway. Transfection with overexpression vectors and siRNA sequences in SK-OV-3 and A2780 cells and incubation for 48 h. Relative expression levels of PTTG1, sGC, PKG2, and PKG1 proteins were detected by western blotting. (Compared between the two groups, *P < 0.05, **P < 0.01, ***P < 0.001, ****P < 0.0001)

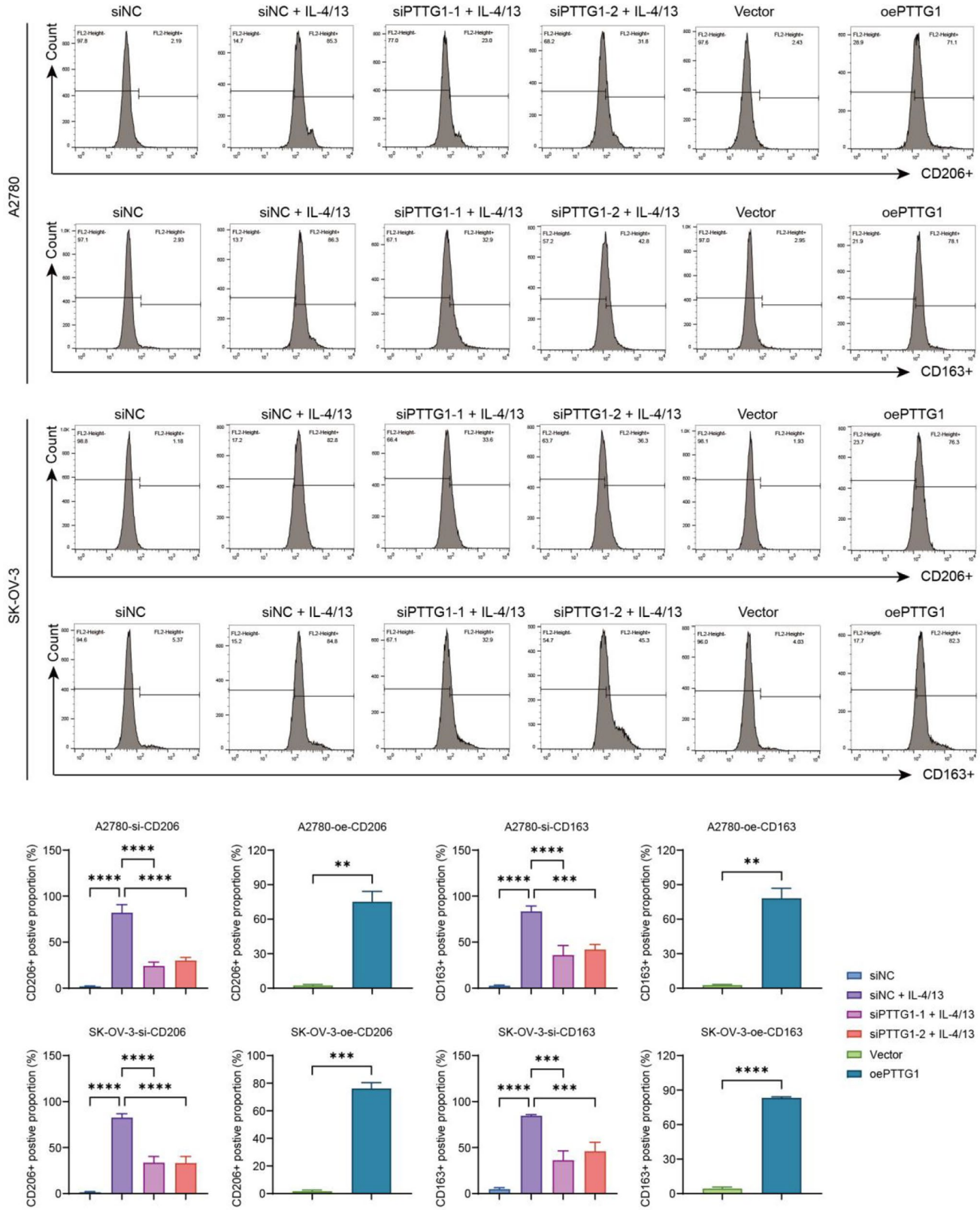

Fig. 5 PTTG1 can induce the positive proportion of CD206 and CD163 in THP-1 cells. Transfection with overexpression vectors and siRNA sequences in SK-OV-3 and A2780 cells and incubation for 48 h. Changes in the proportion of positive cells of CD206 and CD163 by flow cytometry. (Compared between the two groups, *P < 0.05, **P < 0.01, ***P < 0.001, ****P < 0.0001)

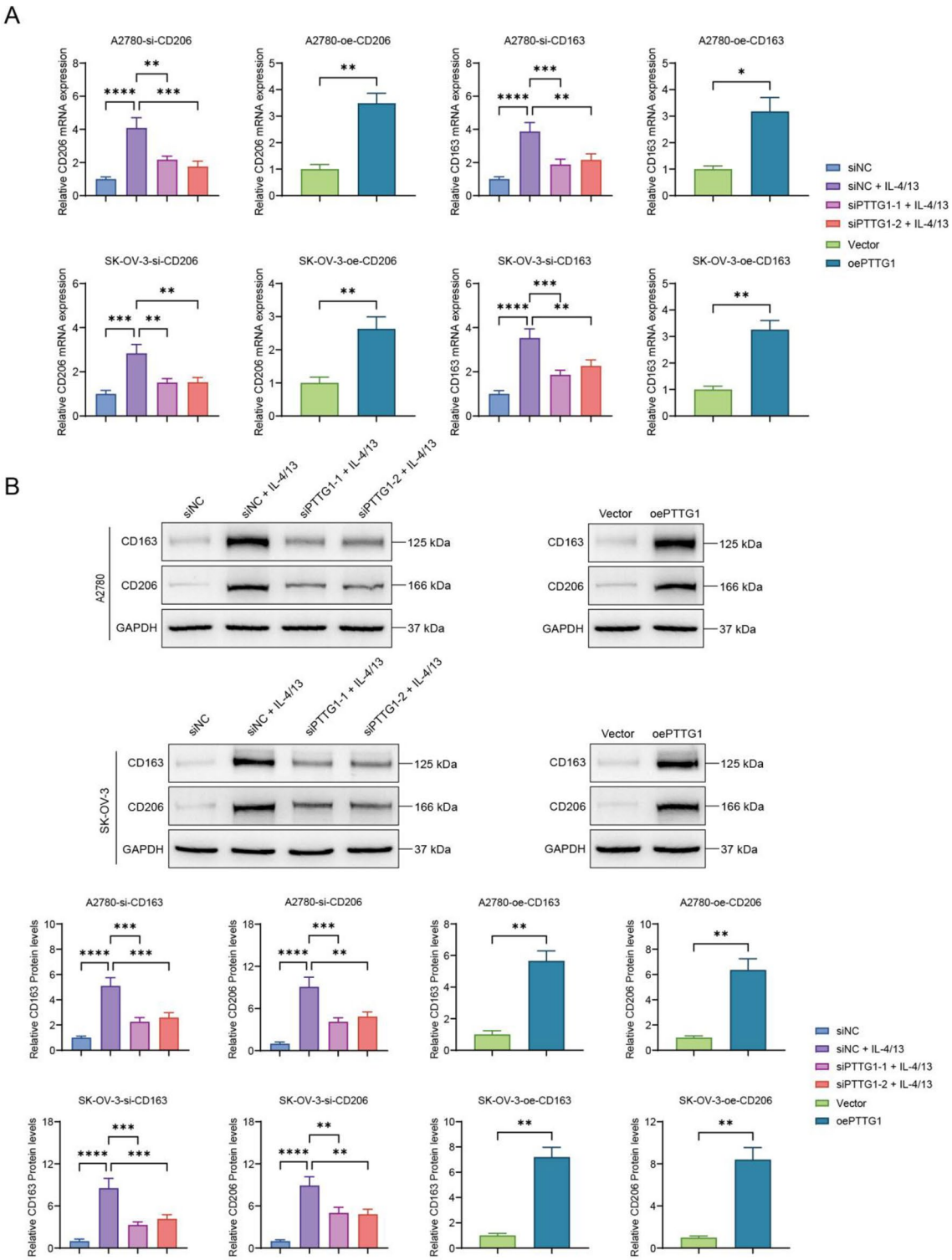

Fig. 6 PTTG1 can enhance the protein and mRNA expression levels of CD206 and CD163 in THP-1 cells. Transfection with overexpression vectors and siRNA sequences in SK-OV-3 and A2780 cells and incubation for 48 h. The relative expression levels of proteins and mRNA of CD206 and CD163 by Western blotting and RT-qPCR. (Compared between the two groups, *P < 0.05, **P < 0.01, ***P < 0.001, ****P < 0.0001)

polarization of macrophages at the metastatic sites of breast cancer cells [35]. This suggests that PTTG1 is a bridging molecule between EMT and macrophage M2 polarization and that its presence may coordinate these two processes and jointly promote breast cancer progression and metastasis. Additionally, it experimentally confirmed that PTTG1 inhibits

the invasion and migration of ovarian cancer cells. Interestingly, the addition of PMA (200 nmol/L) to THP-1 cells significantly reduced the expression of PTTG1, and PMA induced the differentiation of THP-1 cells into M0-type macrophages [36]. This suggests that PTTG1 may be expressed at low levels in M0-type macrophages; however, the expression levels of PTTG1 in M2 and M1 types are unclear. Our study pointed out that an increase in PTTG1 in ovarian cancer cells leads to an increase in M2-type macrophages, but the expression level and influence of PTTG1 in macrophage typing are still unknown, which will be the focus of our subsequent research.

This study for the first time reveals that PTTG1 can serve as a positive target of this pathway, providing a theoretical basis for the development of a synergistic therapy combining"PTTG1 inhibitors and cGMP analogs". Integrating multi—omics data, such as the multi-dimensional map of the genome-epigenome-immune microenvironment of ovarian cancer patients, will help identify the sensitivity of the PTTG1-high-expression subgroup to targeted therapies. Meanwhile, by drawing on the analytical strategies of molecular networks in thymic tumor research, we can deeply explore personalized treatment methods for PTTG1 [37]. In the future, advanced technologies such as compound screening with tools and the use of microfluidic chips to simulate invasion models will be utilized to search for highly effective compounds targeting PTTG1 [38, 39]. In addition, metabolic reprogramming provides the energy and material basis for EMT and simultaneously affects the polarization state of macrophages [40]. M2-type macrophages promote EMT through the secretion of factors, which further impacts the metabolic characteristics of tumor cells [41]. It has been reported that PTTG1 reprograms asparagine metabolism to promote the progression of hepatocellular carcinoma [22], confirming a certain correlation between PTTG1 and cancer metabolism. Our research has verified that PTTG1 can promote the EMT process in ovarian cancer cells and induce M2 polarization of macrophages. However, it remains unclear whether the metabolic process of cancer cells is involved in this process. To further verify this hypothesis, in our subsequent research, we plan to employ multi—omics techniques to comprehensively analyze the impact of PTTG1 on the metabolism of ovarian cancer cells, as well as how these metabolic changes influence EMT and macrophage polarization. This approach could potentially establish a translational closed-loop from mechanism to clinic, propelling ovarian cancer treatment into a new era of multi—target precise intervention. However, our study has certain limitations. First, the experiments were conducted only at the cellular level and not verified in animal models, which may limit the translational application of the results. Second, the specific molecular mechanism underlying PTTG1-induced M2 polarization of macrophages requires further in-depth research. Future studies should construct animal models to simulate the in vivo tumor environment and comprehensively evaluate the role of PTTG1. Overall, this study provides a new direction for research of ovarian cancer and, despite these deficiencies, lays the foundation for subsequent research and has broad development prospects. It is expected to improve the therapeutic effects on ovarian cancer and increase the survival rate and quality of life of patients through intervention targeting PTTG1 in future.

Acknowledgements No.

Author contributions Liang Tian was responsible for Conceptualization, Liyun Liu was responsible for writing the original draft, Chunlou Wang was responsible for data curation, Yan Kong was responsible for the Investigation, Zhigang Miao was responsible for Resources, Qing Yao was responsible for Methodology, He Zhang was responsible for formal analysis, and Yuehong Li was responsible for supervision. All co-authors reviewed and endorsed the final version of the document.

Funding 2023–2024 Cangzhou Science and technology projects (23244102153).

Data availability The datasets produced or examined as part of this investigation were obtained from the lead author upon justified request.

Declarations

Ethics approval and consent to participate Does not apply.

Consent for publication Not applicable.

Competing interests The authors declare no competing interests.

References

1. Feng X, Zahed H, Onwuka J, Callister MEJ, Johansson M, Etzioni R, et al. Cancer stage compared with mortality as end points in randomized clinical trials of cancer screening: a systematic review and meta-analysis. JAMA. 2024;331(22):1910–7. https://doi.org/10.1001/jama.2024.5814.
2. Dalmartello M, La Vecchia C, Bertuccio P, Boffetta P, Levi F, Negri E, et al. European cancer mortality predictions for the year 2022 with focus on ovarian cancer. Ann Oncol Off J Eur Soc Med Oncol. 2022;33(3):330–9. https://doi.org/10.1016/j.annonc.2021.12.007.
3. Webb PM, Jordan SJ. Global epidemiology of epithelial ovarian cancer. Nat Rev Clin Oncol. 2024;21(5):389–400. https://doi.org/10.1038/s41571-024-00881-3.
4. Kuroki L, Guntupalli SR. Treatment of epithelial ovarian cancer. BMJ. 2020;371:m3773. https://doi.org/10.1136/bmj.m3773.
5. Erin N, Grahovac J, Brozovic A, Efferth T. Tumor microenvironment and epithelial mesenchymal transition as targets to overcome tumor multidrug resistance. Drug Resistance Updates Rev Comment Antimicrob Anticancer Chemother. 2020;53:100715. https://doi.org/10.1016/j.drup.2020.100715.
6. May AM, Batoon L, McCauley LK, Keller ET. The role of tumor epithelial-mesenchymal transition and macrophage crosstalk in cancer progression. Curr osteoporos reports. 2023;21(2):117–27. https://doi.org/10.1007/s11914-023-00780-z.
7. Wu M, Mu C, Yang H, Wang Y, Ma P, Li S, et al. 8-Br-cGMP suppresses tumor progression through EGFR/PLC γ1 pathway in epithelial ovarian cancer. Mol Biol Reports. 2024;51(1):140. https://doi.org/10.1007/s11033-023-09037-5.
8. Kong X, Wang JS, Yang H. Upregulation of lncRNA DARS-AS1 accelerates tumor malignancy in cervical cancer by activating cGMP-PKG pathway. J Biochem Mol Toxicol. 2021;35(6):1–11. https://doi.org/10.1002/jbt.22749.
9. Lv Y, Wang X, Li X, Xu G, Bai Y, Wu J, et al. Nucleotide de novo synthesis increases breast cancer stemness and metastasis via cGMP-PKG-MAPK signaling pathway. PLoS Biol. 2020;18(11):e3000872. https://doi.org/10.1371/journal.pbio.3000872.
10. Li W, Yin X, Yan Y, Liu C, Li G. STEAP4 knockdown inhibits the proliferation of prostate cancer cells by activating the cGMP-PKG pathway under lipopolysaccharide-induced inflammatory microenvironment. Int Immunopharmacol. 2021;101(Pt B):108311. https://doi.org/10.1016/j.intimp.2021.108311.
11. Kennel KB, Bozlar M, De Valk AF, Greten FR. Cancer-associated fibroblasts in inflammation and antitumor immunity. Clin Cancer Res. 2023;29(6):1009–16. https://doi.org/10.1158/1078-0432.Ccr-22-1031.
12. Deng X, Wu Q, Li D, Liu Y. Erianin exerts antineoplastic effects on esophageal squamous cell carcinoma cells by activating the cGMP-PKG signaling pathway. Nutr Cancer. 2023;75(6):1473–84. https://doi.org/10.1080/01635581.2023.2205047.
13. Ma J, Shi Y, Lu Q, Huang D. Inflammation-related gene ADH1A regulates the polarization of macrophage M1 and influences the malignant progression of gastric cancer. J Inflamm Res. 2024;17:4647–65. https://doi.org/10.2147/jir.S452670.
14. Rakoczy K, Szymańska N, Stecko J, Kisiel M, Sleziak J, Gajewska-Naryniecka A, et al. The role of RAC2 and PTTG1 in cancer biology. Cells. 2025. https://doi.org/10.3390/cells14050330.
15. Wang Y, Hu J, Chen C, Li Y. PTTG1 induces pancreatic cancer cell proliferation and promotes aerobic glycolysis by regulating c-myc. Open Life Sci. 2024;19(1):20220813. https://doi.org/10.1515/biol-2022-0813.
16. Wei H, Ma Y, Chen S, Zou C, Wang L. Multi-omics analysis identifies PTTG1 as a prognostic biomarker associated with immunotherapy and chemotherapy resistance. BMC Cancer. 2024;24(1):1315. https://doi.org/10.1186/s12885-024-13060-5.
17. Nakachi I, Helfrich BA, Spillman MA, Mickler EA, Olson CJ, Rice JL, et al. PTTG1 levels are predictive of saracatinib sensitivity in ovarian cancer cell lines. Clin Transl Sci. 2016;9(6):293–301. https://doi.org/10.1111/cts.12413.
18. Puri R, Tousson A, Chen L, Kakar SS. Molecular cloning of pituitary tumor transforming gene 1 from ovarian tumors and its expression in tumors. Cancer Lett. 2001;163(1):131–9. https://doi.org/10.1016/s0304-3835(00)00688-1.
19. Daigneault M, Preston JA, Marriott HM, Whyte MK, Dockrell DH. The identification of markers of macrophage differentiation in PMA-stimulated THP-1 cells and monocyte-derived macrophages. PLoS ONE. 2010;5(1):e8668. https://doi.org/10.1371/journal.pone.0008668.
20. Tedesco S, De Majo F, Kim J, Trenti A, Trevisi L, Fadini GP, et al. Convenience versus biological significance: are PMA-differentiated THP-1 cells a reliable substitute for blood-derived macrophages when studying in vitro polarization? Front Pharmacol. 2018;9:71. https://doi.org/10.3389/fphar.2018.00071.
21. Mazan A, Marusiak AA. Protocols for co-culture phenotypic assays with breast cancer cells and THP-1-derived macrophages. J Mammary Gland Biol Neoplasia. 2024;29(1):4. https://doi.org/10.1007/s10911-024-09556-2.
22. Zhou Q, Li L, Sha F, Lei Y, Tian X, Chen L, et al. PTTG1 reprograms asparagine metabolism to promote hepatocellular carcinoma progression. Cancer Res. 2023;83(14):2372–86. https://doi.org/10.1158/0008-5472.Can-22-3561.
23. Inserte J, Garcia-Dorado D. The cGMP/PKG pathway as a common mediator of cardioprotection: translatability and mechanism. Br J Pharmacol. 2015;172(8):1996–2009. https://doi.org/10.1111/bph.12959.
24. Chen L, Zhou X, Deng Y, Yang Y, Chen X, Chen Q, et al. Zhenwu decoction ameliorates cardiac hypertrophy through activating sGC (soluble guanylate cyclase)—cGMP (cyclic guanosine monophosphate)—PKG (protein kinase G) pathway. J Ethnopharmacol. 2023;300:115705. https://doi.org/10.1016/j.jep.2022.115705.
25. Meng L, Lu Y, Wang X, Cheng C, Xue F, Xie L, et al. NPRC deletion attenuates cardiac fibrosis in diabetic mice by activating PKA/PKG and inhibiting TGF-β1/Smad pathways. Sci Adv. 2023;9(31):eadd4222. https://doi.org/10.1126/sciadv.add4222.
26. Wang J, Yang K, Xu L, Zhang Y, Lai N, Jiang H, et al. Sildenafil inhibits hypoxia-induced transient receptor potential canonical protein expression in pulmonary arterial smooth muscle via cGMP-PKG-PPARγ axis. Am J Respir Cell Mol Biol. 2013;49(2):231–40. https://doi.org/10.1165/rcmb.2012-0185OC.
27. Zhou W, Fang D, He Y, Wei J. Correlation analysis of tumor mutation burden of hepatocellular carcinoma based on data mining. J Gastrointest Oncol. 2021;12(3):1117–31. https://doi.org/10.21037/jgo-21-259.

28. Guan R, Zou J, Mei J, Deng M, Guo R. Four-gene signature predicting overall survival and immune infiltration in hepatocellular carcinoma by bioinformatics analysis with RT-qPCR validation. BMC Cancer. 2022;22(1):830. https://doi.org/10.1186/s12885-022-09934-1.
29. Fang C, Cheung MY, Chan RC, Poon IK, Lee C, To CC, et al. Prognostic significance of CD163+ and/or CD206+ tumor-associated macrophages is linked to their spatial distribution and tumor-infiltrating lymphocytes in breast cancer. Cancers (Basel). 2024. https://doi.org/10.3390/cancers16112147.
30. Souriant S, Balboa L, Dupont M, Pingris K, Kviatcovsky D, Cougoule C, et al. Tuberculosis exacerbates HIV-1 infection through IL-10/STAT3-dependent tunneling nanotube formation in macrophages. Cell Rep. 2019;26(13):3586-99.e7. https://doi.org/10.1016/j.celrep.2019.02.091.
31. Moeller JB, Nielsen MJ, Reichhardt MP, Schlosser A, Sorensen GL, Nielsen O, et al. CD163-L1 is an endocytic macrophage protein strongly regulated by mediators in the inflammatory response. J Immunol. 2012;188(5):2399–409. https://doi.org/10.4049/jimmunol.1103150.
32. Orihuela R, McPherson CA, Harry GJ. Microglial M1/M2 polarization and metabolic states. Br J Pharmacol. 2016;173(4):649–65. https://doi.org/10.1111/bph.13139.
33. Cutolo M, Campitiello R, Gotelli E, Soldano S. The role of M1/M2 Macrophage Polarization in Rheumatoid Arthritis Synovitis. Front Immunol. 2022;13:867260. https://doi.org/10.3389/fimmu.2022.867260.
34. Chen X, He X, Xu F, Xu N, Sharifi NH, Zhang P, et al. Fractalkine enhances hematoma resolution and improves neurological function via CX3CR1/AMPK/PPARγ pathway after GMH. Stroke. 2023;54(9):2420–33. https://doi.org/10.1161/strokeaha.123.043005.
35. Xing F, Zhao D, Wu SY, Tyagi A, Wu K, Sharma S, et al. Epigenetic and posttranscriptional modulation of SOS1 can promote breast cancer metastasis through obesity-activated c-met signaling in African-American women. Cancer Res. 2021;81(11):3008–21. https://doi.org/10.1158/0008-5472.Can-19-4031.
36. Chen PY, Yen JH, Kao RH, Chen JH. Down-regulation of the oncogene PTTG1 via the KLF6 tumor suppressor during induction of myeloid differentiation. PLoS ONE. 2013;8(8):e71282. https://doi.org/10.1371/journal.pone.0071282.
37. Zhang X, Zhang P, Cong A, Feng Y, Chi H, Xia Z, et al. Unraveling molecular networks in thymic epithelial tumors: deciphering the unique signatures. Front Immunol. 2023;14:1264325. https://doi.org/10.3389/fimmu.2023.1264325.
38. Chen J, Lin A, Luo P. Advancing pharmaceutical research: a comprehensive review of cutting-edge tools and technologies. Curr Pharm Anal. 2024;21(1):1–19. https://doi.org/10.1016/j.cpan.2024.11.001.
39. Wang Z, Zhao Y, Zhang L. Emerging trends and hot topics in the application of multi-omics in drug discovery: a bibliometric and visualized study. Curr Pharm Anal. 2024;21(1):20–32. https://doi.org/10.1016/j.cpan.2024.12.001.
40. Zhao S, Zhang X, Shi Y, Cheng L, Song T, Wu B, et al. MIEF2 over-expression promotes tumor growth and metastasis through reprogramming of glucose metabolism in ovarian cancer. J Exp Clin Cancer Res. 2020;39(1):286. https://doi.org/10.1186/s13046-020-01802-9.
41. Wang X, Su S, Zhu Y, Cheng X, Cheng C, Chen L, et al. Metabolic reprogramming via ACOD1 depletion enhances function of human induced pluripotent stem cell-derived CAR-macrophages in solid tumors. Nat Commun. 2023;14(1):5778. https://doi.org/10.1038/s41467-023-41470-9.